JOURNAL OF Applied Polymer SCIENCE

Solidification Behavior of High-Density Polyethylene During Injection Molding Process: Enthalpy Transformation Method

Bin Yang, Ji-Bin Miao, Kai Min, Ru Xia, Jia-Sheng Qian, Xing Wang
College of Chemistry and Chemical Engineering, and the Key Laboratory of Environment-Friendly Polymeric Materials of Anhui Province, Anhui University, Hefei 230039, Anhui, People's Republic of China
Correspondence to: B. Yang (E-mail: yangbin@ahu.edu.cn)

ABSTRACT: It was widely established that many end-use properties of the final parts are considerably affected by the macromolecular hierarchical structures formed during the cooling stage of injection molding, especially for crystalline polymers which undergo both solidification and crystallization processes simultaneously. Enthalpy transformation method (ETM) has been demonstrated to give the reasonable descriptions of the temperature profiles for real processing operations (e.g., injection molding, gas-assisted injection molding, and compression molding, etc.) in our previous work. However, to observe the phase-change plateau, where rapid cooling rate is imposed, is not easy in traditional treatments using the enthalpy approach. In this work, "modified cooling curves" (i.e., temperature versus time, plotted in logarithmic scale) at various locations in the mold cavity were found to show similar trend with an obvious turning point indicating the occurrence of phase transition. Mold temperature is more effective in controlling the cooling rate than melt temperature. Turing point of the cooling curves in the plot of ln θ vs. ln t can be used to estimate the minimum cooling time of the injection molding of crystalline polymers. © 2012 Wiley Periodicals, Inc. J. Appl. Polym. Sci. 000: 000–000, 2012

KEYWORDS: enthalpy transformation; injection molding; polyethylene (PE); heat capacity; crystallization

Received 20 May 2012; accepted 21 July 2012; published online
DOI: 10.1002/app.38376

INTRODUCTION

Transient heat-transfer problems with solidification or melting are generally known as the "phase-change problems" or "moving-boundary problems," which were initially raised by Stefan in 1891.[1] Recently, heat-transfer issues of this kind are still of great significance in many engineering applications, e.g., solidification of metallic materials in the mold, cooling of large masses of polymers, as well as freezing of food. Nevertheless, due to the nonlinear nature (i.e., the liquid/solid interface is always moving with the absorption or liberation of the latent heat at the interface[2,3]), to secure the exact solution of those problems is not easy till now.

As one of the widely used fabricating techniques of polymers, injection molding accounts for over 1/3 of all plastics processed in modern industry. Computer-aided engineering (CAE) technology has found wide application in material selection, mold design, analysis of the part defects as well as optimization of the processing parameters for injection molding.[4–7] Attention has been attracted to investigate the heat transfer during the injection moldings of crystalline polymers since early 1990s,[8–10] because the quality and performance of molded parts depend heavily on the selection of operational variables[11–15] during the molding process, especially in the cooling period.

In recent years, numerical solutions turn out to be a useful representation for analyzing the transient heat-transfer issues. For instance, the variational method[16,17] and the enthalpy method[18–23] have been widely applied to solve the multidimensional phase-change problems. More recently, we have successfully employed the enthalpy transformation method (ETM) to obtain the temperature profiles during common processing operations, such as, injection molding,[10,23] gas-assisted injection molding[15,19,21,22,24] as well as compression molding[25] of polyolefins and their blends.

However, the phase-change process can be difficult to observe at locations that have very rapid cooling rate,[26] since the time for phase transition to take place is too short to display in traditional treatments using the enthalpy approach. To further investigate the solidification behavior of crystalline polymers during injection molding process, the cooling curves of temperature versus time were plotted in double-logarithmic scale (as illustrated in Figure 1), and more generalized phenomenon has been observed, that is, a "phase-change zone" or "mushy zone" ($t_1 \sim t_2$, denoted as "Stage II") can be clearly seen in all cases. Besides, the shape of the "modified cooling curve" is found to be independent from the cooling rate. More importantly, there is a turning point (denoted as "TP") within the phase transition

Applied Polymer SCIENCE

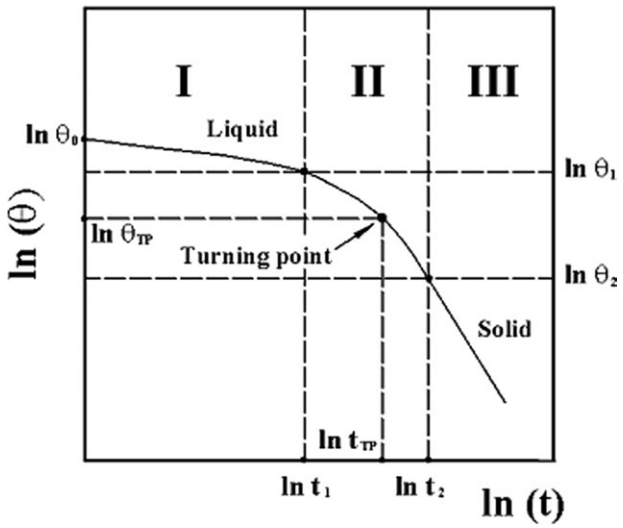

Figure 1. Schematic illustration of the typical cooling curve (in double-logarithmic scale) of crystalline polymers during injection molding. Stage I: liquid-state cooling; Stage II: phase-change process; Stage III: solid-state cooling. θ is the dimensionless temperature defined by $\theta = (T - T_w)/(T_0 - T_w)$, with θ_0, $\theta_1 - \theta_2$, and θ_{TP} denoting the initial temperature, phase-change temperature range (mushy zone), and turning-point temperature, respectively.

zone (i.e., Stage II). TPs at different locations in the cavity can be non-linearly fitted, and can be employed as an estimate of the minimum cooling time for injection moldings of crystalline polymers.

In this article, a new approach was suggested for treating the obtained cooling curves of crystalline polymers during injection molding process. On the basis of our previous work,[10,15,19,21] the graphic solution plotted using this algorithm can better show the whole cooling process of crystalline polymers. The present treatment can better illustrate the solidification behavior (esp., phase transition process) at the positions close to mold wall, where extremely large temperature drop is located. Thus, the objective of this study was to further disclose the physical nature of the heat transfers with phase-change effect of HDPE, which will supply good insights into the formation of various crystalline structures as well as the optimization of processing variables of injection molding process.

EXPERIMENTAL

Material

The material used in this work was high-density polyethylene (HDPE), provided by the Japan Polyethylene (JPE), with its density of 0.953 g/cm^3, and a melt flow rate (MFR) of 0.70 g/10min measured at 190°C under 2.16 kg according to ASTM D1238-98. Detailed material thermal parameters of HDPE were presented in our previous work.[10,19]

Differential Scanning Calorimetry Measurement

Measurement of crystallization behavior was carried out using the differential scanning calorimetry (DSC), Model: Q-200, supplied by TA Instrument, USA, under nonisothermal cooling condition. Sample weighted 5–7 mg was initially heated to 210°C at 10°C/min and kept for 4.0 min to remove the heat history. Then, it was cooled to the ambient temperature at 10°C/min. The phase-change temperature range T_1–T_2 as proposed elsewhere[10] was obtained as 114.1–119.4°C.

Rheological Characterization

Rheological behavior was examined using the melting index (MI) tester, Model: ZRZ1452, supplied by the SANS (Shenzhen) Instrument, P.R. China. Capillary diameter is 2.09 mm, and capillary length is 8.00 mm. The logarithmic apparent viscosity (η_a) of the material shows good linearity with an increase of the inverse absolute temperature (T) under a constant load (2.16 kg) at different temperatures (i.e., 150, 170, 190, 210, and 230°C, respectively), as shown in Figure 2. The melt flow activation energy (E_a) of the material was 24.77 kJ/mol, evaluated using the Arrhenius Equation.

Theoretical Section

The primary assumptions or simplifications used in this work are as follows:

1. Considering the short filling time as compared with the total injection molding cycle, melt-filling stage is neglected,[26] that is, the solidification process starts as soon as the polymer melt contacts the cold metallic wall. Then, the occurrence of a solid/liquid interface ensues.
2. The initial temperature is T_0. There is no contact thermal resistance (CTR) between the polymer melt and the mold wall,[19] i.e., the skin polymer has the mold wall temperature (T_w), which is much below the phase-change temperature of the polymer.
3. The phase transformation of polymers is assumed to take place at certain constant value of T_f (i.e., the "reference temperature"[27,28]), which is defined by $T_f = (T_1 + T_2)/2$, where T_1–T_2 denotes the phase-change temperature range, as proposed previously.[10,21,22]
4. Latent heat (L) is simultaneously released at the solid/liquid interface with the phase-change process. Solid and liquid phases are separated by the interface, whose position will

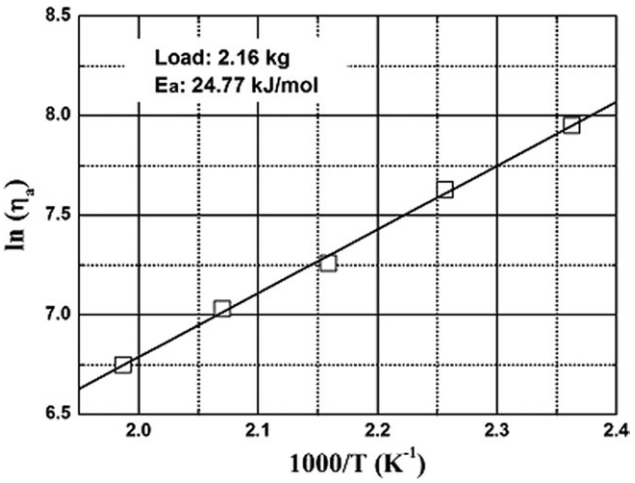

Figure 2. Correlation between apparent viscosity and inverse absolute temperature.

vary with the elapsed time.[26–28] When the two interfaces from the opposite mold walls meet each other at the central plane, the solidification process comes to an end.

5. The thermal parameters of the crystalline plastics, such as thermal conductivity (k), thermal diffusivity (α), heat capacity (C_p), etc., are assumed to be constant within each phase but differ between the phases.[10,23] The inner boundary (i.e., the central plane) of the polymer melt domain was considered adiabatic.[26]

The Energy Equation,[28] coupled with the continuity equation, in the *Cartesian* coordinate system is,

$$\rho \cdot C_P \cdot \frac{DT}{Dt} = \nabla(k \cdot \nabla T) \tag{1}$$

where ρ, k, C_p are density, thermal conductivity and specific heat, respectively. DT/Dt is the material derivative of the temperature T, and ∇ the Hamilton operator. Under constant pressure condition, the enthalpy (E) can be defined as,

$$C_p(T) = \left(\frac{\partial E}{\partial T}\right)_p \tag{2}$$

Temperature can be deemed as a function of E, that is,

$$T(E) = \begin{cases} T_1 + \frac{E}{C_s}, & E \le 0 \quad (3\text{-a}) \\ T_1 + \frac{E \cdot \Delta T}{L + C_f \cdot \Delta T}, & 0 < E < L + C_f \cdot \Delta T \quad (3\text{-b}) \\ T_1 + \frac{E}{C_l} - \frac{L + (C_f - C_l) \cdot \Delta T}{C_l}, & E \ge L + C_f \cdot \Delta T \quad (3\text{-c}) \end{cases}$$

where T_1–T_2 is the phase-change temperature range (i.e., the mushy zone), and $\Delta T = T_2 - T_1$. C_s, C_l are the specific heats of solid phase ($T < T_1$) and liquid phase ($T > T_2$), respectively. C_f is the specific heat within the mushy zone (T_1–T_2), as discussed elsewhere.[10,21] L denotes the latent heat released from the solidification process.

The enthalpy transformation of the Energy Equation can be readily integrated over the entire finite control volumes using *Patankar*'s methodology[28] for control-volume (CV)/finite-difference method (FDM). For the sake of simplicity, the Kirchhoff Temperature (T_{kir}) is introduced[10,18,19,23] and its definition can be given as below,

$$T_{kir} = \Gamma(E) \cdot E + S(E) \tag{4}$$

Γ and S are two parameters that have been detailed elsewhere,[10] the iterative formula of eq. (1) can be expressed as,

$$E_i^{m+1} = E_i^m + \mu \cdot [d_{i-1}^m + d_{i+1}^m - 2 \cdot d_i^m] + \mu \cdot \Delta x \cdot (\rho u) \cdot (E_{i+1}^m - E_i^m) \tag{5}$$

with

$$\mu = \frac{\Delta t}{\rho \cdot \Delta x^2}; \quad d_{i+1}^m = \Gamma_{i+1}^m \cdot E_{i+1}^m + S_{i+1}^m; \quad d_{i-1}^m = \Gamma_{i-1}^m \cdot E_{i+1}^m + S_{i-1}^m; \quad d_i^m = \Gamma_i^m \cdot E_i^m + S_i^m \tag{6}$$

The definite conditions are correspondingly discretized as follows,

$$\text{Initial condition}: E_i^0 = C_l \cdot (T_0 - T_1) + \Delta T \cdot (C_f - C_l) + L; \quad i = 1, 2, 3, \cdots n \tag{7}$$

$$\text{Outer boundary}: E_1^m = C_s \cdot (T_w - T_f); \quad m = 0, 1, 2, \cdots \tag{8}$$

$$\text{Inner boundary}: E_n^m = E_{n-1}^m; \quad m = 0, 1, 2, \cdots \tag{9}$$

Besides, because of the nature of the Energy Equation in explicit form, the above definite problem has stable and convergent numerical solutions when the following criterion[18,27] could be satisfied,

$$0 < \frac{k_s \cdot \Delta t}{\rho \cdot C_s \cdot \Delta x^2} \le 0.5 \tag{10}$$

When the E field is determined from the above iterative procedures, the temperature field can then be easily obtained from eq. (3). The detailed derivation process and iterations of the above algorithms have been presented elsewhere[10] and are omitted here.

RESULTS AND DISCUSSION

Temperature Profiles Under Various Cooling Conditions

The temperature profiles of HDPE during the whole cooling stages of injection molding under three cooling conditions (i.e., Case A: $T_0 = 190°C$, $T_w = 20°C$; Case B: $T_0 = 210°C$, $T_w = 40°C$; Case C: $T_0 = 210°C$, $T_w = 60°C$) were obtained using the above enthalpy transformation technique. The temperature profiles from 10 to 100 s after the cession of melt filling under various processing variables were depicted, as shown in Figure 3. For simplicity, normalized distance was used and defined by $X = x/b$, i.e., where X is the spatial coordinate along the x-axis in dimensionless form and b is the reference length (designated as half the part thickness[9,27]). There are two horizontal imaginal lines (i.e., $T = 110°C$ and $T = 120°C$), which indicate the mushy region or the phase transition zone of polyethylene cooled from the melt state.[10,19,23]

In Figure 3, the position dependence of temperature is evident. To be specific, locations close to mold wall (say, $X = 0.1$–0.3) have the relatively low temperature, while the inner locations (say, $X = 0.8$–1.0) have high temperature in all cases. The distances between the temperature profiles at a given position can be deemed as an estimate of the cooling rates.[19] It is clear that the cooling rate in Case A appears higher than that in Case B, by comparing the temperature profiles at identical time. Exactly speaking, it takes about 60 s for the melt to decrease to the phase-change temperature range (T_1–T_2) at the location of $X = 0.8$ in Cases B and C, while only 40 s in Case A. Remarkable difference in cooling rates under both cases can be observed within a later stage of cooling (e.g., $t > 60$ s), for example, at $X = 0.8$, it takes nearly 100 s to complete the phase-change process in Case C, as compared with those in Cases A and B (both less than 80 s). Therefore, it can be seen that the average cooling rate ranks as, Case A > Case B > Case C. In short, conclusion can be drawn that solidification (non-isothermal

Applied Polymer SCIENCE

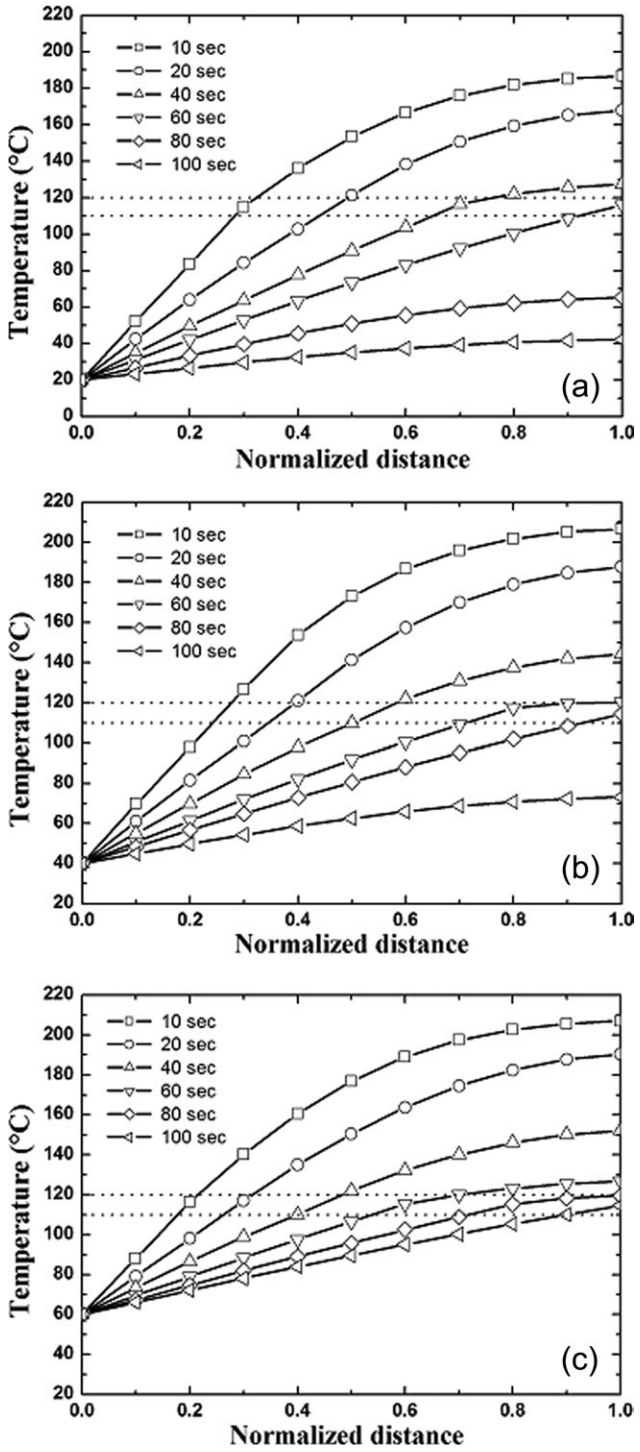

Figure 3. Temperature profiles across the part thickness during injection molding process of HDPE: (a) T_0= 190°C, T_w = 20°C; (b) T_0 = 210°C, T_w = 40°C; (c) T_0 = 210°C, T_w = 60°C.

crystallization) of HDPE will vary greatly with the processing conditions, and it is the differences in the cooling rates that is a key factor dictating the hierarchical structures in the injection-molded parts of crystalline polymers, e.g., polyethylene, polypropylene, and so forth.[12,13,15,29–31]

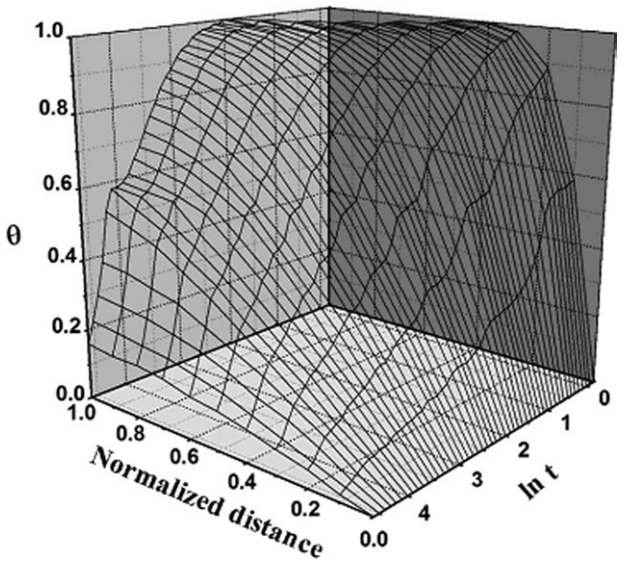

Figure 4. Three-dimensional plot showing the temperature field during the injection molding process of HDPE under the cooling condition T_0 = 190°C and T_w = 20°C.

Figure 4 presents the three-dimensional distribution of the temperature field as a function of location (X) and cooling time (t) under the cooling condition of T_0 = 190°C, T_w = 20°C. For better comparison, the temperature is given in the form of θ, the dimensionless temperature[10,19,24] which is defined by $\theta = (T - T_w)/(T_0 - T_w)$. It can be seen that the temperature falls rapidly to the mold temperature at X = 0, where the polymer contacts the metallic wall; while the temperature decreases slowly in the inner location (e.g., X = 0.8–1.0) and a plateau of phase-change can be found (around ln t = 4). This agrees well with the fact that a typical cooling process of the crystalline plastics undergoes three stages: the liquid-phase cooling, the phase transition, as well as the solid-phase cooling. However, as stated earlier, not all locations can display the temperature hold

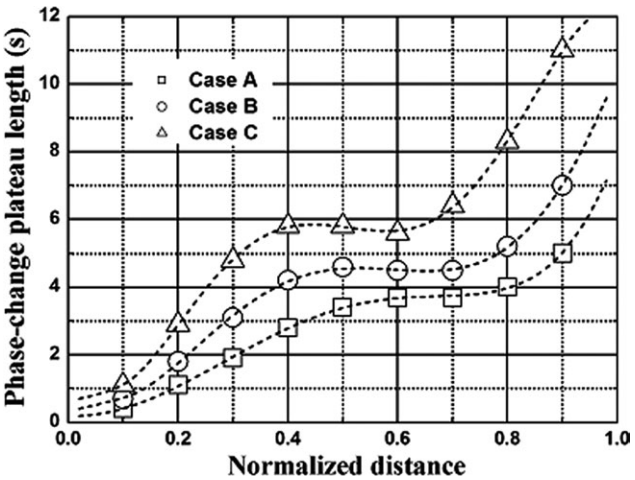

Figure 5. Length of phase-change plateau as a function of normalized distance under various cooling conditions. The dotted lines are plotted to guide the eyes.

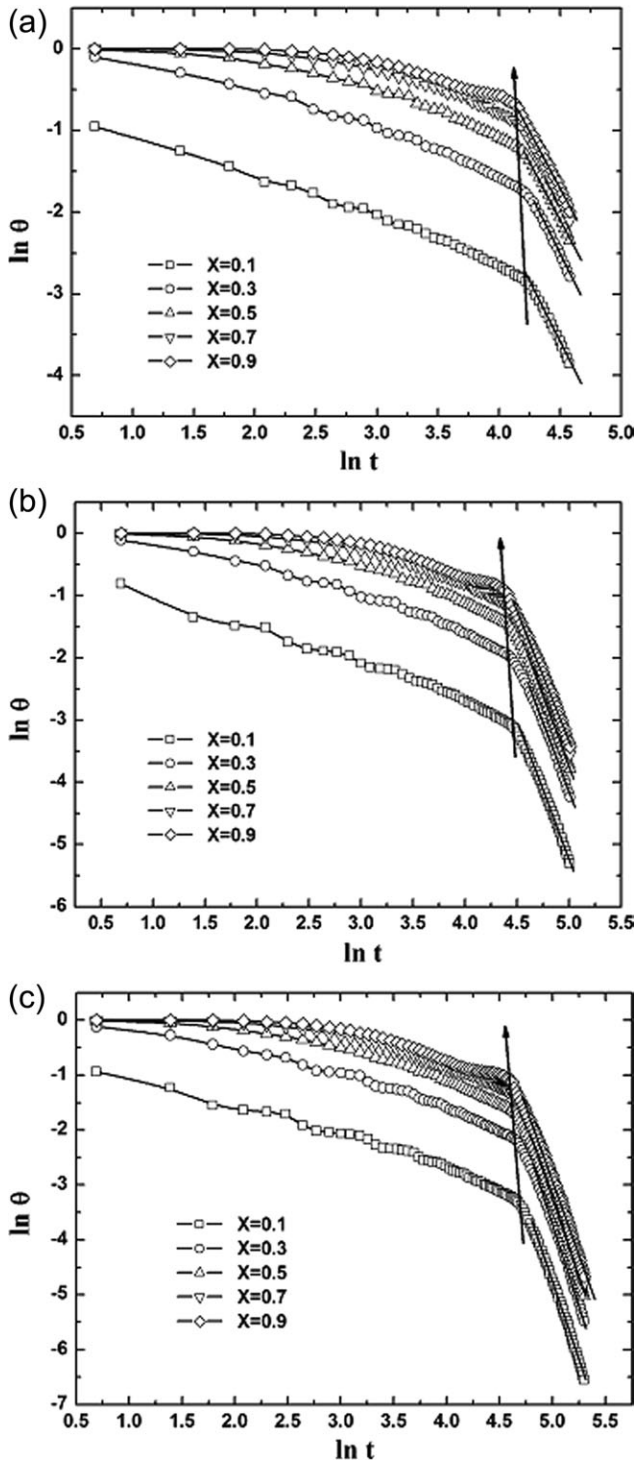

Figure 6. Logarithmic dimensionless temperature (ln θ) versus logarithmic cooling time (ln t) at various locations during injection molding process: (a) $T_0 = 190°C$, $T_w = 20°C$; (b) $T_0 = 210°C$, $T_w = 40°C$; (c) $T_0 = 210°C$, $T_w = 60°C$.

(an isothermal platform), which is a characteristic phenomenon indicating the occurrence of phase transition.[32,33] The temperature hold is primarily attributed to the rate of heat liberated from the crystallization process being the same as that taken away by the cold mold.[26,32] As a result, only one cooling stage can be observed for the positions near the mold wall, since the latent heat released from the phase-change process can be easily transferred away to the cold mold wall because of the high thermal conductivity of the metallic mold and the relatively high temperature difference between the polymer melt and the cold mold. Thus, no redundant heat can be accumulated and no phase-change plateau can be displayed in those regions.

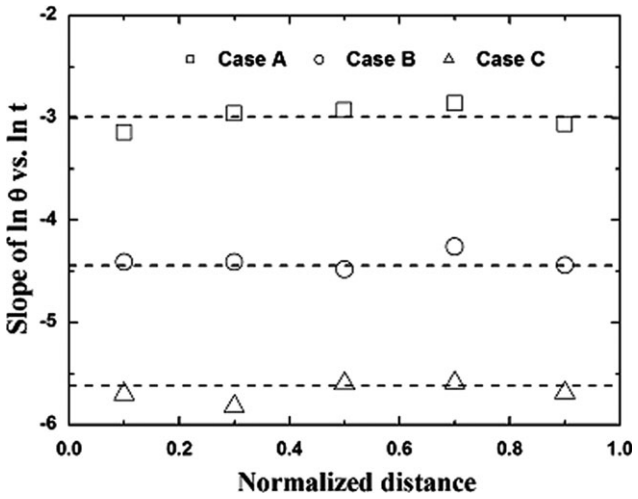

Figure 7. Slope of ln θ vs. ln t during solid-state cooling stage as a function of normalized distance under various cooling conditions.

Figure 5 shows the length of phase-change plateau as a function of normalized distance. It is easy to see that the farther away from the mold wall, the longer the plateau of phase-change extends. Locations that are quite near mold wall have plateau length of less than 1 s, which is the primary reason why the phase transition process is difficult to observe. From the comparison of phase-change plateau, Case C has the longest length, which also indicates that the rate of cooling should rank as, Case C < Case B < Case A. Considering the fact that Cases A

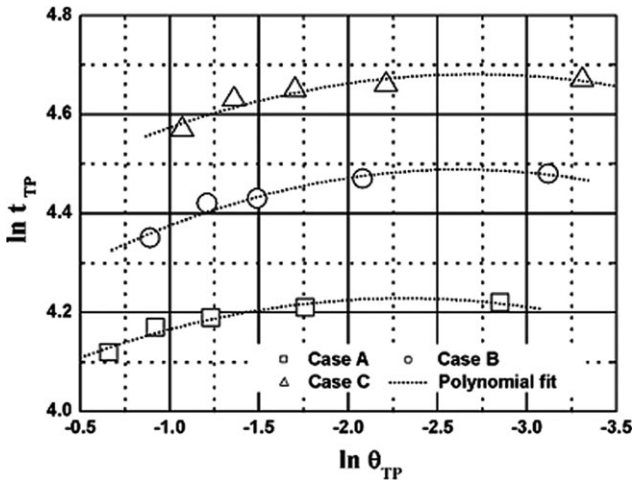

Figure 8. Correlation between temperature and cooling time of turning-points (TPs) under various cooling conditions. The dotted lines are the non-linear fit for respective cooling condition.

Applied Polymer SCIENCE

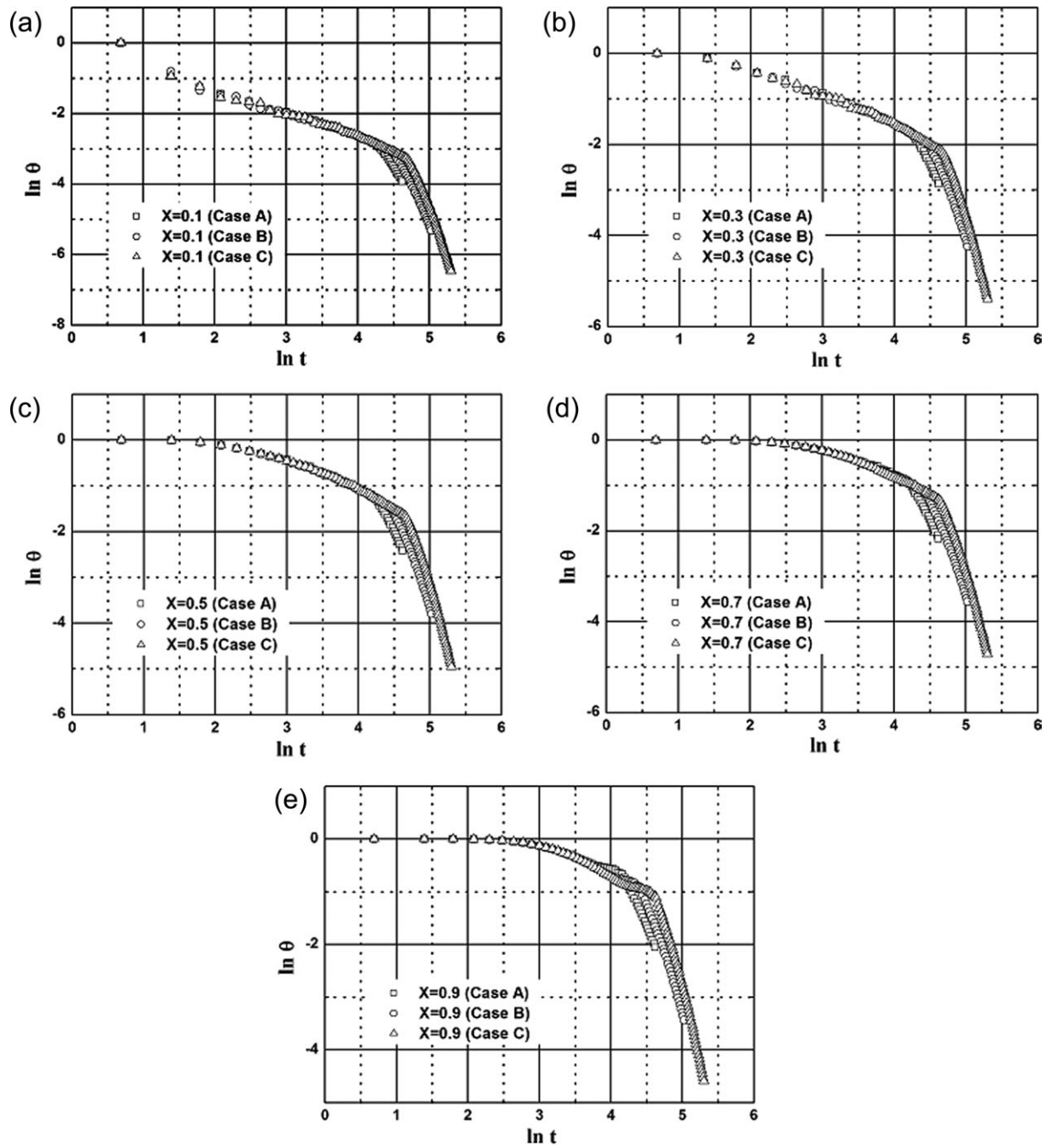

Figure 9. Comparisons of logarithmic dimensionless temperature (ln θ) versus logarithmic cooling time (ln t) at different locations under various cooling conditions: (a) $X = 0.1$; (b) $X = 0.3$; (c) $X = 0.5$; (d) $X = 0.7$; (e) $X = 0.9$.

and B share the same initial temperature difference ($T_0 - T_w$), which is known as the driving force of thermal conduction, Case A has higher cooling rate than Case B, which indicates that the mold temperature (T_w) is more effective in controlling the cooling rate than the melt temperature (T_0).

Solidification Behaviors and Prediction of Cooling Time

Figure 6 presents the relation between logarithmic dimensionless temperature (ln θ) and logarithmic time of cooling (ln t) across the part thickness direction under various processing conditions. It can be easily seen that the "modified cooling curves" show similar shape with a turning point separating each curve into two sections, i.e., liquid-state and solid-state cooling stages, respectively. With an increase of position from $X = 0.1$ to $X = 0.9$ (i.e., from outer region to inner region), the cooling curve becomes higher, indicating slower rate of cooling. It should be noted that in this treatment, all locations can display clear phase-transition process (characteristic of the turning point), which quite differs from traditional treatments with the cooling curves (cf. Figure 4). As the cooling rate increases (i.e., near the wall, say, $X = 0.1$), phase-change balance occurs at a relatively low temperature, which corresponds to a faster crystallization

rate required to balance the rate of heat removal from the polymer melt.[33–35] Since the crystallization takes place much faster, the time over which the plateau exists becomes much shorter. This is also consistent with our earlier discussion.

From $X = 0.1$ to $X = 0.9$, the viscosity (η) and thermal conductivity (k) of the melt decrease with increasing temperature, which makes it more difficult for the heats (sensible heat and latent heat associated with crystallization[10,26]) to be immediately transferred away via thermal conduction. Thus, the cooling curves with respect to inner regions ($X = 0.7-0.9$) seem quite close to each other. Moreover, it is interesting that the solid-state cooling stage of all cooling curves show good linearity. Linear fit is carried out and the results are shown in Figure 7. It was found that the slope of ln θ versus ln t can be a constant for a given cooling condition. The slope value ranks as, Case A > Case B > Case C, which is the same as the rank of cooling rate.

Figure 8 shows correlation between ln t_{TP} and ln θ_{TP} of turning points in each cooling curve, with the respective data taken from Figure 6. The time for the melt to achieve the same temperature (say, ln $\theta_{TP} = -2.0$) ranks as, Case C > Case B > Case A (cf. Figure 8). Nonlinear curve fitting was performed using ORIGIN 8.0, the results of 2nd order polynomial fits (with $R^2 > 0.970$ in all cases) are listed as below:

$$\textbf{Case A}: \ln t_{TP} = 4.034 - 0.169 \cdot (\ln \theta_{TP}) - 0.037 \cdot (\ln \theta_{TP})^2 \quad (11a)$$

$$\textbf{Case B}: \ln t_{TP} = 4.193 - 0.225 \cdot (\ln \theta_{TP}) - 0.043 \cdot (\ln \theta_{TP})^2 \quad (11b)$$

$$\textbf{Case C}: \ln t_{TP} = 4.412 - 0.203 \cdot (\ln \theta_{TP}) - 0.037 \cdot (\ln \theta_{TP})^2 \quad (11c)$$

$$\textbf{Generalized Equation}: \ln t_{TP} = 4.2 - 0.2 \cdot (\ln \theta_{TP}) - 0.04 \cdot (\ln \theta_{TP})^2 \quad (12)$$

From the above eq. (11a-11c), a more generalized equation can be established and expressed as eq. (12). The cooling time of the injection molding process can be thus evaluated when θ_{TP} is replaced by θ_f, which is defined by $\theta_f = (T_f - T_w)/(T_0 - T_w)$. The calculated t_{TP} could be used as an estimate of the minimum cooling time of injection molding, which indicates that the average temperature falls to T_f, and only solid state exists in the part. The predicted cooling times for Cases A, B, and C are at least 73.7 s, 76.3 s, and 78.1 s, respectively.

Figure 9 compares the cooling curves at different locations (from $X = 0.1$ to $X = 0.9$) under various processing variables. It can be noted that the initial stages (liquid-state cooling) agrees well with each other under different cooling conditions, and the major difference is located after the occurrence of turning point. In general, higher cooling rate (e.g., Case A) will lead to higher temperature of phase-change balance but shorter t_{TP}. It can also be concluded that polymer crystallizes at relatively low temperature (as compared with T_f) with increasing cooling rate, and the time within which phase-change plateau extends is shortened due to faster crystallization rate, which is required to balance the rate of heat removal from the polymer melt.[8,23]

Last but not the least, coincidence of data during initial (liquid-state) cooling stage for all cases indicates that initial temperature difference ($T_0 - T_w$) hardly influences the cooling rate of HDPE (cf. Figure 9). Nevertheless, when the melt arrives at the temperature range of crystallization, the value of ($T_f - T_w$), which determines the solid-state cooling rate, will also determine the average cooling rate in the end. This can be the reason why T_w exerts more influence on controlling the cooling rate than T_0, which has also been reported previously.[23] The current analysis of solidification behavior of crystalline polymers can supply good insight into the formation mechanisms of various hierarchical structures in the injection-molded parts.

CONCLUSIONS

In this work, we further explore the solidification behavior of HDPE during the injection molding process on the basis of our previous research. The comparison among three cooling conditions (denoted as Cases A, B, and C, respectively) discloses the reason why the mold temperature (T_w) is more effective in controlling the cooling rate than the melt temperature (T_0). "Modified cooling curves" in the plot of ln θ versus ln t clearly indicate the phase-change process (typical of an isothermal plateau) regardless of the cooling rate, which facilitates the investigation on the solidification and crystallization behaviors of the polymer cooled from the melt state. A generalized equation, which describes the correlation between the time (t_{TP}) and the temperature (θ_{TP}) with respect to the turning point (TP), can be established. More importantly, the equation can be adopted to estimate the minimum cooling time of injection moldings of crystalline polymers [cf. eq. (12)] when θ_{TP} is replaced by θ_f. In short, the present work will supply good insights into the formation of various crystalline structures as well as the optimization of processing variables of injection molding process.

ACKNOWLEDGMENTS

This work was financially supported by the Key Research Project of Anhui Provincial Department of Education (No. KJ2012A011, KJ2011z015), the Ph.D. Research Fund of Anhui University (No. 02303319-0128), the Doctoral Program of Higher Education of China (No. 20113401110003) as well as the "211 Project" of Anhui University. Mr. B. Yang would also like to thank Dr. Long Wang (Sichuan University) for his kind assistance in the verification of the calculated results during the preparation of this contribution.

REFERENCES

1. Crank, J. Free and Moving Boundary Problems; Clarendon Press: Oxford, **1984;** Chapter 2.
2. Carslaw, H. S.; Jaeger, J. C. Conduction of Heat in Solids, 2nd ed.; Clarendon Press: Oxford, **1986;** Chapter 5.
3. Goodman, T. R.; Shea, J. J. *J. Appl. Mech.* **1960,** *27*, 16.
4. Tutar, M.; Karakus, A. *J. Polym. Eng.* **2009,** *29*, 355.
5. De Santis, F.; Pantani, R.; Speranza, V.; Titomanlio, G. *Ind. Eng. Chem. Res.* **2010,** *49*, 2469.
6. Hassan, H.; Regnier, N.; Pujos, C.; Defaye, G. *J. Appl. Polym. Sci.* **2009,** *114*, 2901.
7. Hassan, H.; Regnier, N.; Lebot, C.; Pujos, C.; Defaye, G. *Appl. Thermal. Eng.* **2009,** *29*, 1786.

8. Bai, Y.; Yin, B.; Fu, X. R.; Yang, M. B. *J. Appl. Polym. Sci.* **2006,** *102*, 2249.
9. Hassan, H.; Regnier, N.; Le Bot, C.; Defaye, G. *Int. J. Thermal. Sci.* **2010,** *49*, 161.
10. Yang, B.; Fu, X. R.; Yang, W.; Huang, L.; Feng, J. M.; Yang, M. B. *Polym. Eng. Sci.* **2008,** *49*, 1707.
11. Speranza, V.; Vietri, U.; Pantani, R. *Macromol. Res.* **2011,** *19*, 542.
12. Katti, S. S.; Schultz, J. M. *Polym. Eng. Sci.* **1982,** *22*, 1001.
13. Huang, L.; Yang, W.; Yang, B.; Yang, M. B.; Zheng, G. Q.; An, H. N. *Polymer* **2008,** *49*, 405.
14. Zhang, K.; Liu, Z. Y.; Yang, B.; Yang, W.; Lu, Y.; Wang, L.; Sun, N.; Yang, M. B. *Polymer* **2011,** *52*, 3871.
15. Wang, L.; Yang, B.; Yang, W.; Sun, N.; Yin, B.; Feng, J. M.; Yang, M. B. *Coll. Polym. Sci.* **2011,** *289*, 1661.
16. Bondarev, V. A. *Int. J. Heat Mass Transfer* **1997,** *40*, 3487.
17. Gorla, R. S. R.; Canter, M. S.; Pallone, P. J. *Heat Mass Transfer* **1998,** *33*, 439.
18. Cao, Y.; Faghri, A.; Chang, W. S. *Int. J. Heat Mass Transfer* **1989,** *32*, 1289.
19. Yang, B.; Fu, X. R.; Yang, W.; Liang, S. P.; Sun, N.; Hu, S.; Yang, M. B. *Macromol. Mater. Eng.* **2009,** *294*, 336.
20. Crowley, A. B. *Int. J. Heat Mass Transfer* **1978,** *21*, 215.
21. Yang, B.; Fu, X. R.; Yang, W.; Liang, S. P.; Hu, S.; Yang, M. B. *Polym. Eng. Sci.* **2009,** *49*, 1234.
22. Liang, S. P.; Yang, B.; Fu, X. R.; Yang, W.; Sun, N.; Hu, S.; Yang, M. B. *J. Appl. Polym. Sci.* **2010,** *117*, 729.
23. Tao, S. P.; Fu, X. R.; Yang, M. B.; Yu, R. Z. *Acta Polym Sin.* **2005,** *1*, 8.
24. Wang, L.; Yang, W.; Yang, B.; Sun, N.; Yang, M. B. *Plast. Rubber Compos.* **2010,** *39*, 385.
25. Tang, X. G.; Yang, W.; Shan, G. F.; Yang, B.; Xie, B. H.; Yang, M. B.; Hou, M. *Coll. Polym. Sci.* **2009,** *287*, 1237.
26. Yang, B.; Fu, X. R.; Yang, W.; Sun, N.; Hu, S.; Lu, Y.; Yang, M. B. *J. Macromol. Sci. Phys.* **2010,** *49*, 734.
27. Cho, S. H.; Sunderland, J. E. *J. Heat Transfer* **1969,** *91c*, 421.
28. Özisik, M. N. Heat Conduction; Wiley: New York, **1980; Chapter 10.**
29. Zheng, G. Q.; Huang, L.; Yang, W.; Yang, B.; Yang, M. B.; Liu, C. T.; Li, Q.; Shen, C. Y. *Polymer* **2007,** *48*, 5486.
30. Yang, B.; Yang, M. B.; Wang, W. J.; Zhu, S. P. *Polym. Eng. Sci.* **2012,** *52*, 21.
31. Sun, N.; Yang, B.; Wang, L.; Yang, W.; Zhang, K.; Yang, M. B. *Polym. Plast. Technol. Eng.* **2011,** *50*, 804.
32. Kamal, M. R.; Lafleur, P. G. *Polym. Eng. Sci.* **1986,** *26*, 103.
33. Supaphol, P.; Spruiell, J. E. *J. Polym. Sci. B: Polym. Phys.* **1998,** *36*, 681.
34. Mandelkern, L.; Glotin, M.; Benson, R. A. *Macromolecules* **1981,** *14*, 22.
35. Hu, S.; Yang, W.; Liang, S. P.; Yang, B.; Yang, M. B. *J. Macromol. Sci. Phys.* **2009,** *48*, 1084.